

Superexchange liquefaction of strongly correlated lattice dipolar bosons

Ivan Morera,^{1,2,3} Rafał Oldziejewski,^{4,5,*} Grigori E. Astrakharchik,⁶ and Bruno Juliá-Díaz^{1,2}

¹*Departament de Física Quàntica i Astrofísica, Facultat de Física, Universitat de Barcelona, E-08028 Barcelona, Spain*

²*Institut de Ciències del Cosmos, Universitat de Barcelona, ICCUB, Martí i Franquès 1, E-08028 Barcelona, Spain*

³*Institute for Theoretical Physics, ETH Zurich, 8093 Zurich, Switzerland*

⁴*Max Planck Institute of Quantum Optics, 85748 Garching, Germany*

⁵*Munich Center for Quantum Science and Technology, Schellingstrasse 4, 80799 Munich, Germany*

⁶*Departament de Física, Universitat Politècnica de Catalunya, Campus Nord B4-B5, E-08034 Barcelona, Spain*

Optical lattices with dipolar bosons provide a unique platform for fundamental studies of the extended Bose-Hubbard model. The interplay between anisotropic long-range interaction, strong on-site repulsion and periodic confinement give rise to unexpected phases of matter that have not been explored so far in experiments. We propose a mechanism that stabilizes quantum liquids in strongly interacting dipolar gases in a one-dimensional optical lattice. The mechanism is based on the enhanced role of the superexchange processes close to a self-bound Mott insulator state. To support this finding, we contrast our perturbative calculations with full density-matrix renormalization group simulations and characterize the properties of different phases of the system. Finally, we analyze the speed of sound of the model that exhibits a non-trivial behavior owing to the breaking of Galilean invariance. We argue that an experimental detection of this unknown quantum liquid could provide a fingerprint of the superexchange process and open intriguing possibilities of investigating non-Galilean invariant liquids.

Introduction. The first proposal [1] and subsequent observations of ultra dilute quantum liquids in Bose-Bose mixtures [2–4] and dipolar bosons [5–9] have triggered renewed interest in beyond mean-field effects and quantum fluctuations [10]. In the already well-established picture, quantum droplets emerge as the ground state of a weakly interacting system with both attraction and repulsion between particles when the corresponding mean-field contributions nearly cancel each other giving way to zero-point energy fluctuations — the so-called Lee-Huang-Yang (LHY) term [11–13]. The liquefaction is even more robust in lower dimensions owing to enhanced quantum fluctuations [14–20]. Remarkably, one-dimensional dipoles may acquire liquid properties even for strongly correlated particles when the LHY term loses its applicability [21, 22]. Another interesting platform for studying microscopic foundations of quantum liquid formation comprises one-dimensional optical lattices, where such a mechanism has been studied for Bose-Bose mixtures [23, 24].

Ultracold atoms in optical lattices may as well serve as a quantum simulator of the Hubbard model that plays a vital role in our understanding of strongly correlated solid-state materials. In particular, the Hubbard model at strong coupling displays superexchange processes which can be employed to simulate different quantum magnetic systems [25–29]. The recent experimental progress with atoms possessing strong magnetic moments, like Dy, has led to the first realization of the extended Bose-Hubbard model (eBH) [30]. Due to both the non-local and anisotropic character of dipolar interaction, the eBH potentially exhibits a much richer phase diagram than the standard BH model. Moreover, tun-

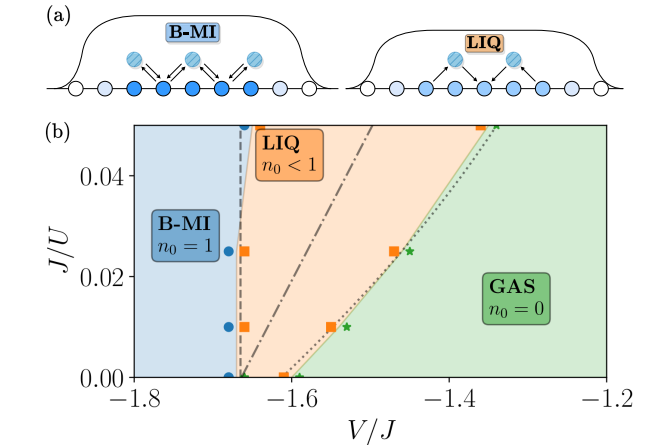


FIG. 1. Panel (a): Schematic representation of a density profile in self-bound Mott insulator (B-MI) having unit filling and liquid drop (LIQ) in which particles are bound but holes are present. Arrows indicate the different superexchange processes through doublon formation. Panel (b): Phase diagram for dipolar bosons in a one-dimensional optical lattice. Different phases can be characterized by their respective equilibrium densities n_0 . We encounter a gaseous phase (GAS), a liquid one, and a self-bound Mott-insulator. Dashed and dotted-dashed lines denote respectively LIQ-to-B-MI and GAS-to-LIQ transitions obtained in perturbation theory. Dotted line indicates the formation of a bound state (dimer) in the two-body problem.

ability of on-site interaction via Feshbach resonances in ultracold setups allows studying the interplay between local and non-local interaction and the presence of a lattice in so-far unexplored regimes.

In this Letter, we theoretically predict and investigate

an unconventional microscopic mechanism of liquid formation for a system confined to a one-dimensional optical lattice with strong on-site repulsion — in the vicinity of the Tonks-Girardeau limit (TG) — and long-range attraction. Notably, we show that the appearance of superexchange processes liquefies the gas state close to an insulator phase transition giving rise to a novel quantum droplet for moderate and large system sizes. Furthermore, we analyze the speed of sound for different phases present in the system. We observe changing behavior as a result of the interplay between interactions and breaking of the Galilean invariance in lattice systems.

Setup and model. We consider a one-dimensional (1D) system of ultracold dipolar bosons loaded to a deep optical lattice comprising N_s sites. The corresponding Hamiltonian is given by an extended Bose-Hubbard (eBH) model,

$$\hat{H} = -J \sum_{i=1}^{N_s} \left(\hat{b}_i^\dagger \hat{b}_{i+1} + \text{h.c.} \right) + \frac{U}{2} \sum_{i=1}^{N_s} \hat{n}_i (\hat{n}_i - 1) + V \sum_{i < j=1}^{N_s} \frac{\hat{n}_i \hat{n}_j}{|i - j|^3}, \quad (1)$$

with hopping J , on-site interaction U and dipolar strength V . Importantly, it is possible to tune U/J and V/J separately in experiments with 1D optical lattices [31], for example, by using Feshbach resonances and adjusting the polarization angle of the magnetic moment in the system. Thus, all the phases considered in this Letter can be accessed in a quasi-1D setting for ^{162}Dy atoms alike in [31], see the Supplemental Material for details [32]. A typical transverse length of a trapping potential in current experiments with ultracold gases $\sigma_\perp \approx 50$ nm [31] is much smaller than a typical lattice spacing $a \approx 500$ nm. We thus use pure dipolar interaction in 1D instead of the effective potential for quasi-1D geometries [33] as the latter includes corrections only at short distances of the order of σ_\perp . Hereafter, we fix the length scale $a = 1$ to the lattice spacing. In the following, we study the ground state of the system described by Hamiltonian (1) for large values of the on-site repulsion ($U/J \gg 1$) by developing perturbation theory and performing numerical simulations.

Insulator instability. We start by investigating an impenetrable lattice TG gas ($U/J \rightarrow \infty$) perturbed by an attractive dipolar interaction ($|V| \sim J$). We develop an analytical theory by assuming a lattice TG state $|\psi_{\text{TG}}\rangle$ at a density $n = N/N_s$ and calculating the effective equation of state (EoS) perturbatively as $E = \langle \psi_{\text{TG}} | \hat{H} | \psi_{\text{TG}} \rangle$. The resulting energy per particle $e \equiv E/N$ reads $e = e_J + e_V$, where

$$e_J = -2J \sin(n\pi)/(n\pi), \quad (2)$$

$$e_V = V \left(\zeta(3)n + \frac{\zeta(5)}{2n\pi^2} - \frac{1}{4n\pi^2} [\text{Li}_5(e^{2i\pi n}) + \text{Li}_5(e^{-2i\pi n})] \right),$$

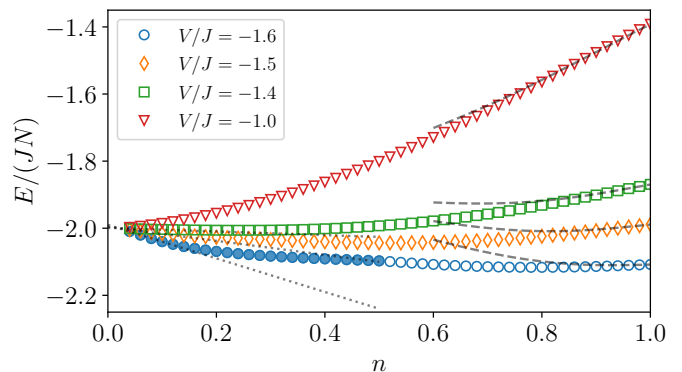


FIG. 2. Equation of state of dipolar bosons in a one-dimensional optical lattice for different values of the dipolar strength V/J with a fixed on-site interaction $U/J = 20$. Filled symbols denote inhomogeneous solutions. Dashed lines show the Tonks-Girardeau perturbative result [32]. Dotted line shows the behavior expected for a lattice soliton solution [34]. A liquid forms when the equation of state shows a minimum at some finite value of density n_0 with the energy per particle $E/N_0 < -2J$, see $V/J = -1.4, -1.5, -1.6$ curves. A gas occurs when the minimum is located at zero density with the energy per particle $E/N > -2J$, see $V/J = -1.0$ curve.

indicate the kinetic energy of the fermionized bosons and the dipolar interaction energy accordingly. We also introduce the polylogarithm function $\text{Li}_\beta(n)$ of order β .

The minimum in the energy is reached at zero density when $V/J < V_{\text{B-MI}}/J$. At this critical value, the minimum of the EoS jumps to unit density. This signals a first order transition to an insulator state. Furthermore, the insulator state has a lower energy per particle than the free particle energy $-2J$. It is thus a self-bound state, to which we refer as a self-bound Mott insulator (B-MI). The threshold of the B-MI state is defined by the condition that the energy per particle at unit filling equals the free energy per particle $e(n=1) = -2J$, giving the critical value of the long-range interaction $V_{\text{B-MI}}/J = 2/\zeta(3)$. B-MI states feature complete incompressibility. Thus in finite systems they become completely localized exhibiting compact density profiles with a saturated density corresponding to strictly one particle per site $n = 1$ (see Fig. 1). Although the density profile for these states bears similarity to quantum droplets, quantum correlations are completely suppressed in the B-MI case (see also Fig. 3). Therefore, one should not consider them as genuine liquids. In fact, they can be related to phase-separated states in spin systems [35].

Importantly, lattice physics significantly differs from what one expects to find in a continuous analogue of the described system. In the 1D continuum, the addition of attractive dipolar interaction to TG gas leads to the collapse of the system as the quantum fluctuations cannot compensate for the diverging dipolar attraction. The feature of a lattice is that it provides a natural regular-

ization of the problem since, for hard-core particles, the maximum density allowed is fixed by the lattice spacing ($n \leq 1$) [36]. Notice, however, that genuine self-bound droplets in the TG limit for quasi-1D dipolar bosons, where the existence of transverse structure regularizes short-range divergence, were predicted recently [21].

Superexchange processes and liquefaction. The mechanism lying behind B-MI formation is based on a near cancellation between the effective repulsion coming from the kinetic energy of lattice hard-core particles and the long-range dipolar attraction. This scenario resembles a droplet formation for weakly interacting bosons with cancelling mean-field contributions and stabilization due to beyond mean-field LHY terms. In the following, we study the effects of relaxing the hard-core condition in our system.

We consider penetrable bosons with large but finite on-site interaction $U/J \gg 1$. We thus move away from the TG limit that opens the possibility of next-to-nearest neighbor hopping through a virtual intermediate process of two bosons occupying the same site — the so-called superexchange process. Explicitly, this extra contribution e_U to the total energy e can be derived using the effective fermionic Hamiltonian within the second-order degenerate perturbation theory [32, 37], and it reads:

$$e_U = -\frac{4J^2}{U}n \left(1 - \frac{\sin(2\pi n)}{2\pi n} \right). \quad (3)$$

Note that the superexchange correction effectively introduces additional attraction of order $J^2/U \ll 1$ in the system for all densities.

Remarkably, by inspecting the modified EoS of the ground state, we encounter a gas to liquid transition close to the B-MI boundary owing entirely to the emerging superexchange process, which diminishes on-site repulsion. The found liquid phase is characterized by a negative energy per particle smaller than for the free case $E/N < -2J$ and a finite equilibrium density $0 < n_0 < 1$ (see Fig. 1). By increasing the attractive long-range coupling, the density saturates with one particle per site, and consequently, the system enters the B-MI state.

Notably, the discovered mechanism of liquefaction in the strongly-correlated regime bears certain similarities with the one vastly studied in the opposite limit of weak interactions. As therein, quantum liquids appear due to the subleading terms when dominating contributions of opposite signs cancel each other. Nonetheless, contrary to the LHY term as a small beyond mean-field effect, the superexchange correlations occur for strongly interacting systems well beyond the mean-field applicability.

Numerical methods. So far, we have treated the model defined by Eq. (1) in the $U/J \gg 1$ limit perturbatively. In the following, we support our analytic theory with unbiased numerical results obtained by using density-matrix renormalization group (DMRG) method.

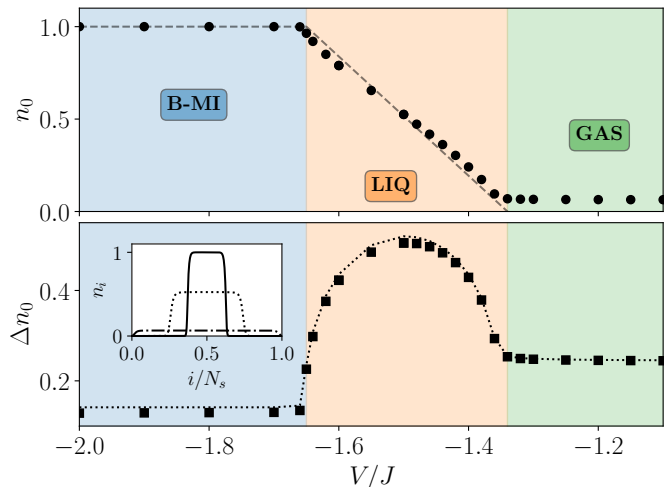


FIG. 3. Density and its variance as a function of the dipolar strength for a large value of the on-site interaction $U/J = 20$. Top panel: Saturated density n_0 (circles). Dashed line: unit filling, $n_0 = 1$ (B-MI); zero filling, $n_0 = 0$ (GAS); linear interpolation (LIQ). We have performed o.b.c numerical simulations up to a density $n = 50/800$. Bottom panel: Particle number variance $\Delta n_0^2 = \langle \hat{n}_0^2 \rangle - \langle \hat{n}_0 \rangle^2$ (squares). Dotted line denotes the particle number variance obtained in a TG-like state, see main text. Inset: Characteristic density profiles obtained for $V/J = -1.8$ (B-MI), $V/J = -1.5$ (LIQ) and $V/J = -1.3$ (GAS).

To calculate various properties of different phases exhibited by the considered system, we performed simulations with $N_s = 100 - 800$ lattice sites and $N = 50 - 100$ particles. To obtain the density dependence, we imposed periodic boundary conditions on Hamiltonian (1) and employed DMRG. We find an excellent agreement between these results and the ones obtained with the infinite-DMRG method where the homogeneous solution is mechanically stable. To obtain the quantum droplets in Fig. 3, we used open boundary conditions ensuring that the system size does not affect the profiles. Further details on the numerical method are reported in the Supplementary Material [32].

Equilibrium properties. To benchmark the perturbative EoS, we have numerically calculated the ground-state energy of Hamiltonian (1) for different strengths of the long-range interaction V/J keeping fixed a large but finite on-site interaction U/J , see Fig. (2). In the case of larger densities ($n \gtrsim 0.8$), an excellent agreement is found for any value of the long-range interaction, especially when approaching the unit filling limit $n = 1$ owing to suppressed quantum correlations. For smaller densities ($n \lesssim 0.5$), the effective EoS deviates significantly, as it does not include the presence of few-body bound states. In DMRG simulations, we always observe that the appearance of the liquid phase coincides with the formation of a two-body bound state in the system, see Fig. 1. Details on solving the two-body problem are

given in [32]. In the few-body limit, the equation of state is well approximated by a lattice soliton solution [34] $\frac{E}{N} + 2J \sim \frac{(N-1)}{2}\epsilon_b$ with ϵ_b being the two-particle bound-state energy, see Fig. 2. The appearance of the lattice soliton shows that the long-range effects of the dipolar interaction at small densities can be absorbed into the binding energy ϵ_b .

The EoS allows one to differentiate three distinct phases in the system, see Fig. 2. The gaseous phase features a minimum in the EoS at zero density $n_0 = 0$ and a positive energy per particle compared to the free case $e > -2J$. On the other hand, the liquid and B-MI phases are characterized by negative binding energies $e < -2J$ in the minimum. The B-MI phase features a saturated density $n_0 = 1$ while the equilibrium density of a liquid ranges within $0 < n_0 < 1$. Accordingly, the liquid state is compressible while the B-MI is not.

One of the qualitative differences between the predictions of perturbative theory and DMRG results is the presence of a narrow liquid phase in the TG limit $J/U = 0$. This liquid state is sandwiched between the gas and B-MI phases for $V_{\text{MI}} < V < -1.61J$, see Fig. 1. The weakest attraction, for which the liquid forms, is defined by the existence of a two-body bound state. Remarkably, for the dipolar interaction, the formation of a two-body bound state does not coincide with the formation of a self-bound MI state in the many-body problem for $J/U = 0$, in contrast to faster decaying potentials. We thus relate the presence of the liquid phase to the long-range nature of the dipolar interaction. We shall explore further the character of this liquid phase in a future work.

The equilibrium properties differ dramatically among the various phases, as shown in Fig. 3. The equilibrium density ranges from $0 < n_0 < 1$ in the liquid phase and saturates to $n_0 = 1$ in the B-MI phase. DMRG simulations result in density profiles that do not fill the entire lattice for these phases, contrary to the gaseous state. Moreover, the value of the saturated density agrees excellently with the equilibrium density found from the EoS. Its value increases almost linearly for the growing attractive long-range interaction in the liquid phase. Upon reaching the B-MI phase, the equilibrium density saturates to $n_0 = 1$ and becomes independent of the dipolar coupling.

Another important observable pertains to the particle variance $\Delta n_0 = \sqrt{\langle \hat{n}_0^2 \rangle - n_0^2}$, as it quantifies the fluctuations of density and probes the structure of pair correlations. In particular, it vanishes in the gas phase (due to vanishing equilibrium density) and in the B-MI phase becomes of order J/\sqrt{U} . We find that the maximal value of Δn is reached in the liquid phase close to half-filling $n_0 \sim 1/2$. Fascinatingly, the lattice TG model captures the particle variance model well and provides a precise analytic description, see Fig. 3.

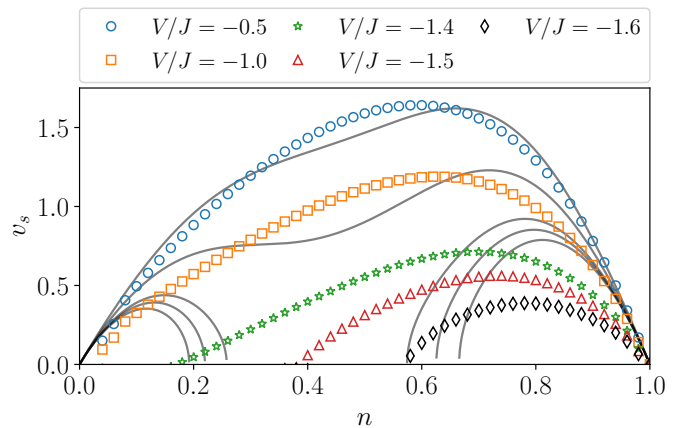


FIG. 4. Speed of sound as a function of the density for different values of the dipolar interaction V/J for a fixed on-site interaction $U/J = 20$. Lines show the perturbative result.

Speed of sound. Due to the experimental ability to measure the speed of propagation of holons and doublons in optical lattices [38], we investigate the speed of sound in our model. Generally, addition of an attractive (dipolar) interaction softens the phononic excitations as compared to hard-core gas, thus reducing the sound velocity. Simultaneously, the presence of a lattice has strong consequences on sound propagation [39, 40] and other transport properties [41], as can be traced to the loss of Galilean invariance in the lattice. These two effects sum up producing a non-trivial dependence of the sound on the density. To obtain the speed of sound c_s , we calculate static structure factor $S(k)$, compute the compressibility κ_s from the EoS, and employ the non-Galilean version of the Feynman relation [32, 42], $S(k) = \hbar \kappa_s c_s n k / 2$ applicable for small momenta. In Fig. 4, we present the speed of sound as a function of the density for different values of the long-range coupling. For weak dipolar attraction, the speed of sound decreases above half-filling and reaches zero at unit filling, signaling the transition to a MI state. As the dipolar strength increases, a liquid state forms, and the sound velocity also vanishes at spinodal density $n_s \leq 1$. Zero value of c_s signals that the homogeneous solution becomes unstable. Finally, when approaching the B-MI phase, the speed of sound nears zero for any value of density showing that no stable homogeneous solution exists for $|V| > |V_{\text{B-MI}}|$.

For an analytical estimation of the speed of sound, we employ the non-Galilean invariant Luttinger liquid theory [39, 40]. Within it, the sound velocity $v_s = \sqrt{v_N v_J}$ is determined through the phase v_J and density v_N stiffnesses. Assuming the TG state, we explicitly compute the response of the system and the speed of sound [32], see Fig. 4. For weak dipolar attraction, we note a good agreement between the perturbative theory and exact numerics. As the strength of attraction is increased, the analytical approach predicts the appearance of a spinodal

point, albeit at an incorrect value of density. Additionally, we report a qualitative difference emerging at small densities where perturbative theory predicts a finite value of the speed of sound, which is in stark contrast with numerical results, where no stable homogeneous solution exists for $n \leq n_s$. We associate this discrepancy with the formation of molecules at small densities, which is completely overlooked in the perturbative description.

Discussion and outlook. Our work showcases rich physics exhibited by dipolar bosons in 1D optical lattices. In particular, our results open a new avenue for studying the interplay between non-local attractive interaction and the superexchange processes related to strong on-site repulsion leading to a novel quantum liquid state. Namely, the direct observation of such lattice liquid will be a telling fingerprint of the superexchange's very presence. Recently one-dimensional dipolar bosonic systems have been produced experimentally [31], where the dipolar strength can be tuned by changing the polarization angle between the dipoles.

In parallel, these lattice liquids can be a platform for studying the intriguing properties of non-Galilean invariant liquids with long-range interactions and, for example, their implications on superfluidity.

Additionally, potential connections between the investigated liquid phases and the magnetic orders expected in the underlying effective spin model also warrant further exploration. Finally, our theory could also be applied to fermionic systems with density correlated hopping and attractive long-range interactions.

Acknowledgements. This work has been funded by Grant No. PID2020-114626GB-I00 from the MICIN/AEI/10.13039/501100011033 and by the Ministerio de Economía, Industria y Competitividad (MINECO, Spain) under grants No. FIS2017-84114-C2-1-P and No. FIS2017- 87534-P. We acknowledge financial support from Secretaria d'Universitats i Recerca del Departament d'Empresa i Coneixement de la Generalitat de Catalunya, co-funded by the European Union Regional Development Fund within the ERDF Operational Program of Catalunya (project QuantumCat, ref. 001-P001644). R. O. acknowledges support by the Max Planck Society and the Deutsche Forschungsgemeinschaft (DFG, German Research Foundation) under Germany's Excellence Strategy – EXC-2111 – 390814868.

* Correspondence to: rafal.oldziejewski@mpq.mpg.de

- [1] D. S. Petrov, *Phys. Rev. Lett.* **115**, 155302 (2015).
- [2] C. R. Cabrera, L. Tanzi, J. Sanz, B. Naylor, P. Thomas, P. Cheiney, and L. Tarruell, *Science* **359**, 301 (2018).
- [3] P. Cheiney, C. R. Cabrera, J. Sanz, B. Naylor, L. Tanzi, and L. Tarruell, *Phys. Rev. Lett.* **120**, 135301 (2018).
- [4] G. Semeghini, G. Ferioli, L. Masi, C. Mazzinghi, L. Wolswijk, F. Minardi, M. Modugno, G. Modugno, M. Inguscio, and M. Fattori, *Phys. Rev. Lett.* **120**, 235301 (2018).
- [5] M. Schmitt, M. Wenzel, F. Böttcher, I. Ferrier-Barbut, and T. Pfau, *Nature* **539**, 259 (2016).
- [6] I. Ferrier-Barbut, H. Kadau, M. Schmitt, M. Wenzel, and T. Pfau, *Phys. Rev. Lett.* **116**, 215301 (2016).
- [7] L. Chomaz, S. Baier, D. Petter, M. J. Mark, F. Wächtler, L. Santos, and F. Ferlaino, *Phys. Rev. X* **6**, 041039 (2016).
- [8] I. Ferrier-Barbut, M. Wenzel, F. Böttcher, T. Langen, M. Isoard, S. Stringari, and T. Pfau, *Phys. Rev. Lett.* **120**, 160402 (2018).
- [9] F. Böttcher, M. Wenzel, J.-N. Schmidt, M. Guo, T. Langen, I. Ferrier-Barbut, T. Pfau, R. Bombín, J. Sánchez-Baena, J. Boronat, and F. Mazzanti, *Phys. Rev. Research* **1**, 033088 (2019).
- [10] F. Böttcher, J.-N. Schmidt, J. Hertkorn, K. S. H. Ng, S. D. Graham, M. Guo, T. Langen, and T. Pfau, *Reports on Progress in Physics* **84**, 012403 (2020).
- [11] T. D. Lee, K. Huang, and C. N. Yang, *Phys. Rev.* **106**, 1135 (1957).
- [12] A. R. P. Lima and A. Pelster, *Phys. Rev. A* **84**, 041604 (2011).
- [13] A. R. P. Lima and A. Pelster, *Phys. Rev. A* **86**, 063609 (2012).
- [14] D. S. Petrov and G. E. Astrakharchik, *Phys. Rev. Lett.* **117**, 100401 (2016).
- [15] D. Edler, C. Mishra, F. Wächtler, R. Nath, S. Sinha, and L. Santos, *Phys. Rev. Lett.* **119**, 050403 (2017).
- [16] G. E. Astrakharchik and B. A. Malomed, *Phys. Rev. A* **98**, 013631 (2018).
- [17] P. Zin, M. Pylak, T. Wasak, M. Gajda, and Z. Idziaszek, *Phys. Rev. A* **98**, 051603 (2018).
- [18] T. Ilg, J. Kumlin, L. Santos, D. S. Petrov, and H. P. Büchler, *Phys. Rev. A* **98**, 051604 (2018).
- [19] D. Rakshit, T. Karpiuk, P. Zin, M. Brewczyk, M. Lewenstein, and M. Gajda, *New Journal of Physics* **21**, 073027 (2019).
- [20] M. Edmonds, T. Bland, and N. Parker, *Journal of Physics Communications* **4**, 125008 (2020).
- [21] R. Oldziejewski, W. Górecki, K. Pawłowski, and K. Rzążewski, *Phys. Rev. Lett.* **124**, 090401 (2020).
- [22] S. De Palo, E. Orignac, and R. Citro, arXiv preprint arXiv:2202.12071 (2022).
- [23] I. Morera, G. E. Astrakharchik, A. Polls, and B. Juliá-Díaz, *Phys. Rev. Research* **2**, 022008 (2020).
- [24] I. Morera, G. E. Astrakharchik, A. Polls, and B. Juliá-Díaz, *Phys. Rev. Lett.* **126**, 023001 (2021).
- [25] L.-M. Duan, E. Demler, and M. D. Lukin, *Phys. Rev. Lett.* **91**, 090402 (2003).
- [26] S. Trotzky, P. Cheinet, S. Fölling, M. Feld, U. Schnorrberger, A. M. Rey, A. Polkovnikov, E. A. Demler, M. D. Lukin, and I. Bloch, *Science* **319**, 295 (2008).
- [27] L.-M. Duan, E. Demler, and M. D. Lukin, *Phys. Rev. Lett.* **91**, 090402 (2003).
- [28] T. Fukuhara, A. Kantian, M. Endres, M. Cheneau, P. Schauß, S. Hild, D. Bellem, U. Schollwöck, T. Giamarchi, C. Gross, I. Bloch, and S. Kuhr, *Nature Physics* **9**, 235 (2013).
- [29] P. N. Jepsen, J. Amato-Grill, I. Dimitrova, W. W. Ho, E. Demler, and W. Ketterle, *Nature* **588**, 403 (2020).
- [30] S. Baier, M. J. Mark, D. Petter, K. Aikawa, L. Chomaz, Z. Cai, M. Baranov, P. Zoller, and F. Ferlaino, *Science* **352**, 201 (2016).

- [31] W. Kao, K.-Y. Li, K.-Y. Lin, S. Gopalakrishnan, and B. L. Lev, *Science* **371**, 296 (2021).
- [32] See the Supplementary Material for additional information on the perturbation theory, two-body bound state formation, numerical methods, calculation of the sound velocity in a lattice, and experimental implementation of the model.
- [33] F. Deuretzbacher, J. C. Cremon, and S. M. Reimann, *Phys. Rev. A* **81**, 063616 (2010).
- [34] A. Scott, J. Eilbeck, and H. Gilhøj, *Physica D: Nonlinear Phenomena* **78**, 194 (1994).
- [35] D. Petrosyan, B. Schmidt, J. R. Anglin, and M. Fleischhauer, *Phys. Rev. A* **76**, 033606 (2007).
- [36] Note that this holds in the regime of applicability of the single-band eBH. For very strong attractive dipolar interactions, one may need to include higher bands into consideration.
- [37] M. A. Cazalilla, *Phys. Rev. A* **67**, 053606 (2003).
- [38] M. Cheneau, P. Barmettler, D. Poletti, M. Endres, P. Schauß, T. Fukuhara, C. Gross, I. Bloch, C. Kollath, and S. Kuhr, *Nature* **481**, 484 (2012).
- [39] M. A. Cazalilla, *Journal of Physics B: Atomic, Molecular and Optical Physics* **37**, S1 (2004).
- [40] M. A. Cazalilla, *Phys. Rev. A* **70**, 041604 (2004).
- [41] R. Anderson, F. Wang, P. Xu, V. Venu, S. Trotzky, F. Chevy, and J. H. Thywissen, *Phys. Rev. Lett.* **122**, 153602 (2019).
- [42] K. V. Krutitsky, *Physics Reports* **607**, 1 (2016), ultracold bosons with short-range interaction in regular optical lattices.
- [43] B. Pirvu, V. Murg, J. I. Cirac, and F. Verstraete, *New Journal of Physics* **12**, 025012 (2010).

Supplementary Material for 'Superexchange liquefaction of strongly correlated lattice dipolar bosons'

LATTICE FERMIONS WITH A LONG-RANGE INTERACTION

One can obtain a correct description of relevant features of the system by perturbatively adding an attractive long-range interaction to the non-interacting lattice Fermi gas. By considering the Fermi gas state we can estimate the energy as,

$$\begin{aligned}
 E &= E_K + E_V \quad (S1) \\
 &= -2JN_s \sin(n\pi)/\pi + V \sum_{i<j=1}^{N_s} \frac{\langle \hat{n}_i \hat{n}_j \rangle}{|i-j|^3}.
 \end{aligned}$$

The first term represents the kinetic energy of the lattice Fermi gas that we obtain in the thermodynamic limit $N, N_s \rightarrow \infty$ for a fixed particle density $n = N/N_s$. The second term is the dipolar energy, which can be computed in a perturbative manner by employing Wick's theorem $\langle \hat{n}_i \hat{n}_j \rangle/n^2 = 1 - \sin^2(k_F|i-j|)/(k_F|i-j|)^2$, where we introduce the Fermi momentum $k_F = \pi n$, and we employ $\langle \hat{c}_i^\dagger \hat{c}_j \rangle = \sin(k_F|i-j|)/(\pi|i-j|)$. After some algebraic manipulations, we obtain the total energy per particle,

$$\begin{aligned}
 E/N &= -2J \sin(n\pi)/(n\pi) + V\xi(3)n \quad (S2) \\
 &+ \frac{V\xi(5)}{2n\pi^2} \\
 &- \frac{V}{4n\pi^2} [\text{Li}_5(e^{2i\pi n}) + \text{Li}_5(e^{-2i\pi n})].
 \end{aligned}$$

The liquid phase becomes energetically favorable when the energy per particle is smaller as compared to its value in the gas phase at zero density, that is when $E/N < -2J$. In principle, the attractive long-range interaction lowers the energy per particle and the system will liquefy for a critical value of V/J . Since we deal with hard-core particles, the system cannot have more than one particle per site. This imposes limitations on the equilibrium density, which should lie in the $0 < n_0 \leq 1$ range. Therefore, there is a critical point of the long-range interaction strength for which the equilibrium density of the liquid corresponds to the occupation of one particle per site. In that situation, self-bound Mott insulators appear in finite-size systems while bulk systems exhibit insulator properties and are completely incompressible. The perturbative equation of state Eq. (S2) allows for estimating a critical value for the long-range strength at which the equilibrium density touches one,

$$V_{\text{MI}}/J = 2/\xi(3). \quad (S3)$$

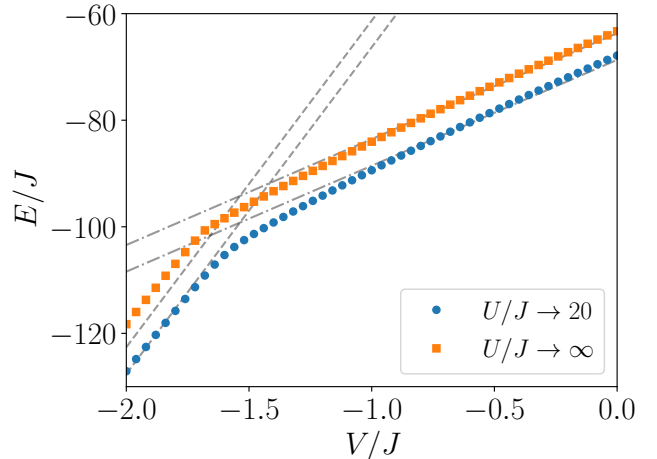


FIG. 1. Energy E of dipolar bosons loaded in a one-dimensional optical lattice as a function of the dipolar strength V for the case of hard-core bosons $U/J \rightarrow \infty$ and a strong but finite on-site interaction $U/J = 20$. The simulations are performed with $N = 50$ particles in a lattice of $N_s = 100$ sites. Perturbative energy calculations for a fixed density $n = 1$ (dashed line) and $n = 0.5$ (dotted-dashed line).

To see the appearance of a liquid phase, we need to obtain $E/N < -2J$ before reaching the self-bound Mott-insulator phase $V > V_{\text{MI}}$. By evaluating the energy per particle at the transition point we obtain $E/N|_{n=1, V=V_{\text{MI}}} = -2J$. Therefore, we see that there is no intermediate regime where a liquid phase can be found with $E/N < -2J$ and $0 < n_0 < 1$. The perturbative equation of state Eq. (S2) predicts a direct transition between a gas and a self-bound Mott-insulator at a strength given by Eq. (S3).

QUASI-TONKS-GIRARDEAU REGIME WITH ON-SITE AND LONG-RANGE INTERACTIONS

After examining the upshots of adding long-range interaction to an ideal Fermi system, we also include the effect of having realistic bosons (not hard-core ones) with strong on-site interaction U . This effect can be taken into account at second order in degenerate perturbation the-

ory in U/J [37], leading to the effective Hamiltonian,

$$\hat{H} = -J \sum_{i=1}^{N_s} \left(\hat{c}_i^\dagger \hat{c}_{i+1} + \text{h.c.} \right) + \frac{2J^2}{U} \sum_{i=1}^{N_s} \left(\hat{c}_{i-1}^\dagger \hat{n}_i \hat{c}_{i+1} + \text{h.c.} \right) - \frac{4J^2}{U} \sum_{i=1}^{N_s} \hat{n}_i \hat{n}_{i+1} + V \sum_{i < j=1}^{N_s} \frac{\hat{n}_i \hat{n}_j}{|i-j|^3}, \quad (\text{S4})$$

where \hat{c}_i^\dagger and \hat{c}_i represent creation and annihilation fermionic operators at site i . The energy of the system is given by,

$$E = E_K + E_V + E_U, \quad (\text{S5})$$

where E_K and E_V are given by Eq. (S2) and the on-site energy reads,

$$E_U/N = -\frac{4J^2}{U} n \left(1 - \frac{\sin(2\pi n)}{2\pi n} \right). \quad (\text{S6})$$

We observe that the reduction of infinite on-site repulsion to a finite one has an attractive effect and $E_U < 0$. Therefore, the quasi-TG fluid is less repulsive than the Fermi fluid for the same long-range coupling. Due to the different density dependence of the energy contributions, the on-site interaction can liquefy the system. Thus, by reducing the on-site interaction, we expect to observe a gas to liquid transition. In the dilute regime $n \ll 1$, the perturbative terms remain small compared to the rest of Eq. (S5). On the other hand, for larger densities they play an important role. In particular, one can observe the non-monotonous behavior of the energy as a function of the density. This will have strong implications on many thermodynamic observables of the quasi-TG liquid such as its compressibility.

To test predictions of the developed perturbative theory, we perform DMRG simulations of Hamiltonian (1) by fixing a number of particles in the system and varying the long-range strength V with a large on-site interaction U , see Fig. 1. When $V < V_{\text{MI}}$, see Eq. (S3), the homogeneous solution is stable and the perturbative calculations with a homogeneous density given by $n = N/N_s$ correctly predict the behavior of the energy of the system as a function of the long-range strength. When it exceeds the critical value $V > V_c$, the homogeneous solution becomes unstable with respect to formation of a self-bound MI which is a droplet with a saturated density $n = 1$. By employing the same perturbative equations for a fixed density $n = 1$, we can also predict the dependence of the self-bound MI energy on the dipolar interaction strength. The abrupt change of the energy as the long-range strength reaches the critical value V_c signals the presence of a first-order phase transition between the homogeneous liquid and an inhomogeneous, completely incompressible self-bound insulator.

THE TWO-BODY PROBLEM

A problem of two dipolar bosons in a one-dimensional lattice can be solved by separating the centre of mass and relative motion and using the following set of states,

$$|\psi\rangle = \frac{1}{\sqrt{N_s}} \sum_{i,j} e^{iQR} \psi_Q(z) |i, j\rangle, \quad (\text{S7})$$

where we introduce the total quasi-momentum Q of a pair, relative $z = i-j$ and total $R = (i+j)/2$ coordinates, a wavefunction of the relative motion $\psi_Q(z)$ and the two particle state $|i, j\rangle = \hat{b}_i^\dagger \hat{b}_j^\dagger |0\rangle$. After inserting Eq. (S7) into Eq. (1), we obtain the equation of motion for the relative wavefunction,

$$E_Q \psi_Q(z) = \sum_{e=\pm 1} -2J \cos(Q/2) \psi_Q(z+e) \quad (\text{S8}) \\ + U \delta(z) \psi_Q(z) + 2V \sum_{n=1}^{N_s} \frac{\delta(|z|-n)}{n^3} \psi_Q(z).$$

Above, we introduce the energy of the pair E_Q that depends parametrically on the quasi-momentum Q . By numerically solving Eq. (S8), we get a spectrum of the system as a function of the pair quasi-momentum presented in Fig. 2. We notice that for large values of the on-site interaction $U \gg J$, there is a critical negative value of the dipolar strength V_c/J , for which a bound state appears in the spectrum. This bound state appears below the two-particle scattering continuum and its energy has a minimum at $Qa = 0$. It is characterized by a negative binding energy E_B/J defined as a difference between the energy of the state and the minimum of the scattering band. For larger negative values of the dipolar strength, more bound states can be found. For the deepest bound state in the system, we compute a typical relative distance between the two particles z^* as a function of the dipolar strength. We observe that after crossing the critical dipolar strength V_c/J , the two particles already localize in adjacent sites. This indicates the local nature of the bound state even though the presence of a long-range dipolar interaction. We conclude that the typical distance between two particles is set by the lattice spacing $z^* \sim a$. We also explore the dependence of the critical dipolar strength V_c/J for bound state formation on the on-site interaction U/J , see Fig. 3. The critical value V_c/J decreases rapidly for small values of the on-site interaction U/J . For larger on-site repulsion, it slowly tends to the critical value $V_c/J \sim -1.61$ in the fermionization limit ($U/J \rightarrow \infty$). This is also the critical dipolar strength obtained for the fermionic case, where the relative wavefunction $\psi_Q(z)$ is completely antisymmetric.

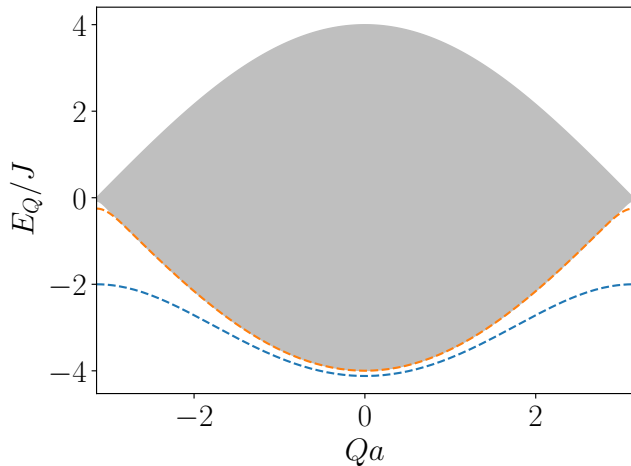


FIG. 2. Energy of two dipolar bosons in a 1D optical lattice as a function of the total quasi-momentum Qa of the pair. The on-site interaction is $U/J = 20$ and the dipolar strength $V/J = -10$. The filled gray region represents the scattering continuum and dashed lines depict bound state solutions.

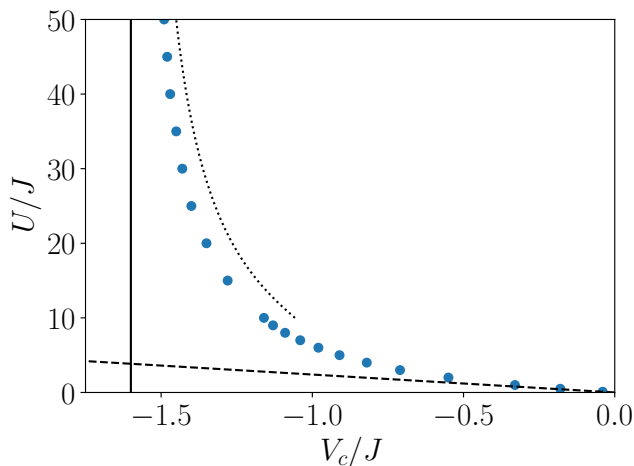


FIG. 3. Critical value of the dipolar strength V_c/J for bound state formation for different values of the on-site interaction U/J . Dashed line represents the critical dipolar strength obtained in the fermionized limit $U/J \rightarrow \infty$.

NUMERICAL METHOD

We employ the standard two-site update DMRG and iDMRG algorithms in order to find the ground state of Hamiltonian (1). In our code, to go beyond the nearest-neighbour interaction and couple two arbitrary distant dipolar bosons, we fit the power-law decaying dipolar interaction with a sum of ten exponential functions [43]. Thus, we are not cutting the range of the interaction in the numerical implementation of our model. To test the MPS representation of the ground state, we have checked

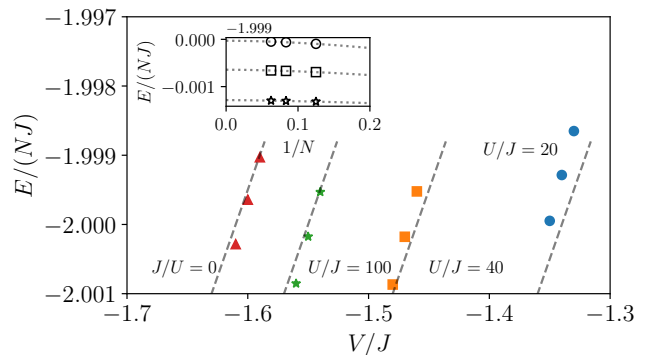


FIG. 4. Main panel: Energy per particle in the thermodynamic limit for a system density $n = 1/10$ as a function of the dipolar strength V/J for different values of on-site interaction U/J . The gas to liquid phase transition occurs when $E/(NJ) = -2$. Dashed lines indicate a two-body decoupling, see the main text. Inset panel: Energy per particle dependence with the number of particles at fixed density for the case of hard-core bosons.

the convergence in terms of the bond dimension χ up to $\chi = 800$. The quantities presented in the main text, such as the energy or particle variance, show a fast convergence with the bond dimension. At the same time, we have implemented a cutoff in the maximum number of bosons per site N_m . Our perturbative theory hints that doublons play a crucial role for the formation of the liquid state. We thus also checked the convergence for the varying cutoff N_m . For the case $U = 20$ and $V = -1.5$, which shows the maximum particle variance (see the main text), we observe an excellent convergence already obtained for $N_m = 3$. The energy and entanglement entropy difference with respect to $N_m = 4$ are $\Delta E = 10^{-7}$ and $\Delta S = 10^{-7}$. Therefore, all the results presented in the main text are performed at $N_m = 3$. The excellent agreement between our perturbative theory and the DMRG results shows that doublons created through superexchange processes are the main mechanism for liquefaction.

GAS TO LIQUID TRANSITION

To detect the gas to liquid phase transition, we study the stability of the homogeneous gas as a function of the interactions for a very small density $n = 0.1$. To fix the density of the system, we impose the periodic boundary conditions on the Hamiltonian and then employ DMRG. For increasing dipolar interaction, the many-body gas state becomes self-bound $E/N < -2J$ and a transition to a liquid phase occurs, see Fig. 4. To ensure the many-body transition, we study the dependence of the energy per particle with the number of particles for fixed density

$n = 1/10$. This allows to extract the thermodynamic limit.

The energy per particle depends almost linearly on the strength of dipolar interactions. This points to a two-body decoupling. All interaction effects can be absorbed in a two-body coupling strength $g_0 = (V - V_0)$, V_0 being the point at which a two-body bound state appears. The energy per particle can be thus estimated as $E/N = \frac{1}{2}g_0n$. Remarkably, this gives a good estimation of the energy per particle close to the liquid to gas transition, see Fig. 4.

PARTICLE VARIANCE

The local particle variance can be directly related with the local pair-correlation function $g_2 = \langle \hat{b}^\dagger \hat{b}^\dagger \hat{b} \hat{b} \rangle / n^2$,

$$\Delta n \equiv \sqrt{\langle \hat{n}^2 \rangle - n^2} = \sqrt{g_2 n^2 + n - n^2}. \quad (\text{S9})$$

By employing the Hellmann-Feynman theorem, the local pair-correlation function can be written as,

$$g_2 = \frac{2}{n^2} \frac{\partial}{\partial U} \left(\frac{E_U}{N_s} \right) = \frac{8J^2}{U^2 n^2} \left(1 - \frac{\sin(2\pi n)}{2\pi n} \right), \quad (\text{S10})$$

which leads to the particle variance,

$$\Delta n \equiv \sqrt{n - n^2 + \frac{8J^2}{U^2} \left(1 - \frac{\sin(2\pi n)}{2\pi n} \right)}. \quad (\text{S11})$$

The particle variance can be used to detect different phases present in the system. The gas to liquid phase transition is characterized by a discontinuity in the first derivative of the local particle variance at equilibrium $\Delta n_0 \sim \sqrt{n_0}$. On the other hand, when crossing the transition from liquid to self-bound Mott-insulator, the particle variance is an analytic differentiable function $\Delta n_0 \sim 2\sqrt{2}J/\sqrt{U} - (n_0 - 1)\frac{8J^2+U}{4\sqrt{2}J\sqrt{U}}$ for any value of finite on-site interaction $U/J \gg 1$. However, it shows a kink at the transition point owing to the presence of a discontinuity of the first derivative of the equilibrium density. In the Tonks-Girardeau limit $U/J \rightarrow \infty$, the particle variance also exhibits a discontinuity in its first derivative $\Delta n_0 \sim \sqrt{1 - n_0}$.

DENSITY AND PHASE RESPONSE

Lattices naturally break Galilean invariance since the particle current is not a conserved quantity in any two-particle collision even though the total quasi-momentum is conserved. This has dramatic consequences on many thermodynamic and transport observables. It also implies that the low-energy Luttinger theory cannot be described by a single parameter but rather needs two distinct phenomenologic parameters. These two parameters

can be introduced by measuring the response of the system to a change in particle number and to a phase shift,

$$v_N = \frac{N_s a}{\pi \hbar} \frac{\partial^2 E}{\partial N^2} \Big|_{N=N_0}, \quad v_J = \frac{\pi N_s a}{\hbar} \frac{\partial^2 E}{\partial \phi^2} \Big|_{\phi=0}. \quad (\text{S12})$$

Notice that for a Galilean invariant system, one parameter is immediately reduced $v_J = v_F$ with the Fermi velocity v_F , fully fixed by the linear density. In that case, the low-energy properties are entirely characterized by the adiabatic compressibility. Instead, for a lattice system, one has to compute both parameters in a microscopic calculation. The low-energy properties of the fluid can be expressed in terms of these parameters,

$$K = \sqrt{\frac{v_J}{v_N}}, \quad v_s = \sqrt{v_J v_N}, \quad (\text{S13})$$

v_s being the speed of sound of the low-energy phonons and K the Luttinger parameter determining the long-range correlations in the fluid. The velocity v_N is inversely proportional to the compressibility of the system showing that the more incompressible the fluid, the larger the velocity v_N . On the other hand, the speed of sound v_s is also affected by the response to phase fluctuations and both v_J and v_N can have an effect on it. The compressibility can already be computed from Eq. (S5) leading to the density response,

$$v_N = 2J \sin(\pi n) + \frac{8J^2}{\pi U} (\cos(2\pi n) - n \sin(2\pi n) - 1) + \frac{V}{\pi} [2\xi(3) + \text{Li}_3(e^{-2i\pi n}) + \text{Li}_3(e^{2i\pi n})] \quad (\text{S14})$$

To compute the response to phase fluctuations, we also performed a perturbative calculation imposing twisted boundary conditions $\hat{c}_{i+N_s} = e^{i\phi} \hat{c}_i$. In the thermodynamic limit, this leads to a phase shift in the correlation function $\langle \hat{c}_i^\dagger \hat{c}_j \rangle = e^{i\phi|i-j|/N_s} \sin(k_F|i-j|)/(\pi|i-j|)$. By employing Wick's theorem, we can again obtain perturbatively the dependence of the energy on the phase ϕ . After some manipulations, the phase response is given by,

$$v_J = 2J \sin(\pi n) + \frac{8J^2}{\pi U} [2 \sin^2(\pi n) - \pi n \sin(2\pi n)] \quad (\text{S15})$$

In our perturbative calculation, we observe that the dipolar interaction does not lead to any modification of the phase response in the system. This is already expected since it is a density-density interaction, and it only affects the compressibility of the system.

Combining our calculations, we are able to calculate the speed of sound in the lattice TG with a non-local interaction,

$$v_s = 2J \sin(\pi n) - \frac{16J^2}{U} n \sin(\pi n) \cos(\pi n) + \frac{V}{2\pi} [2\xi(3) + \text{Li}_3(e^{-2i\pi n}) + \text{Li}_3(e^{2i\pi n})]. \quad (\text{S16})$$

FEYNMAN RELATION IN A LATTICE

In absence of an optical lattice, the Feynman relation provides an upper bound to the lower branch of the excitation spectrum $E(k)$, in terms of the static structure factor $S(k)$ according to $E(k) \leq \hbar^2 k^2 / [2mS(k)]$. The upper bound becomes exact when excitations are reduced to a single mode. It happens, for example, at low momenta where phonons are strongly populated. This also corresponds to the regime in which the Luttinger liquid applies. The lattice analogue of the Feynman relation can be found by employing the non-Galilean invariant Luttinger theory. The long-distance decay of density-density correlation is dictated by the Luttinger parameters Eq. (S13),

$$\langle \delta n_i \delta n_j \rangle \sim \frac{K}{2\pi^2 |i-j|^2}, \quad (\text{S17})$$

The pair correlation function is defined as,

$$g = 1 + \frac{1}{n^2} \langle \delta n_i \delta n_j \rangle, \quad (\text{S18})$$

and static structure factor is obtained from it by using Fourier transform according to

$$S(k) = 1 + n \sum_j e^{ikj} (g - 1). \quad (\text{S19})$$

The long-distance decay Eq. (S17) results in a linear low-momentum dependence of the static structure factor as,

$$S(k) = \frac{K}{2n\pi} k. \quad (\text{S20})$$

By defining the compressibility and using Eq. (S13), we obtain the following relations

$$\kappa_s^{-1} = n^2 \frac{\partial \mu}{\partial n} = \hbar \pi v_N n^2 = \frac{\hbar \pi v_s n^2}{K}, \quad (\text{S21})$$

between the Luttinger parameter K , the speed of sound v_s and the inverse compressibility κ_s^{-1} . By inserting these relations into the low-momentum expansion of the static structure factor we obtain,

$$S(k) = \frac{\hbar \kappa_s v_s n}{2} k. \quad (\text{S22})$$

The above is the lattice analogue of Feynman relation in continuum. By knowing the low-momentum behavior of the static structure factor and the compressibility of the system, we can calculate the speed of sound and hence the phononic part of the excitation spectrum, $E(k) = \hbar k v_s$.

To recover the continuum limit, one just has to set $v_J = v_F = \pi n$, which sets the inverse compressibility $\kappa_s^{-1} = \hbar v_s^2 n$ and thus obtaining

$$S(k) = \frac{k}{2v_s}, \quad (\text{S23})$$

which corresponds to the Feynman relation in the continuum with $m = 1$. In the continuum, one thus has a direct relationship between compressibility and the speed of sound. Namely, when a system becomes less compressible, its speed of sound increases.

EXPERIMENTAL IMPLEMENTATION

Ultracold atoms provide an ideal experimental platform to realize a strongly interacting lattice bosonic system with an attractive long-range interaction. Specifically, dipolar bosons loaded to a one-dimensional optical lattice are perfect candidates to produce a long-range interaction with a power-law decay. One can obtain a pure dipolar interaction by assuming that the characteristic transverse length σ_\perp is much smaller than the lattice spacing in the longitudinal direction a_x , which is fulfilled in recent experiments [31]. Moreover, the on-site interaction can also be tuned by employing Feshbach resonances. Finally, the strength of the dipolar interaction can be tuned by changing the polarization angle θ between the dipoles,

$$V = \frac{C_{dd}}{4\pi} \frac{1 - 3 \cos^2(\theta)}{a_x^3}, \quad (\text{S24})$$

being C_{dd} the dipolar coupling.

Considering the recent quasi one-dimensional setting for ^{162}Dy atoms [31] ($C_{dd} \approx (9.93\mu_B)^2 \mu_0$) with $\sigma_\perp = 952a_0$, a_0 being the Bohr radius, $V_\perp = 30E_\perp$ and $E_\perp/\hbar = 2\pi \times 2.24\text{kHz}$ and a longitudinal optical lattice of lattice spacing $a_x = 532\text{ nm}$ with a height $V_x = 14E_x$, one can cross all the phases encountered in the main text by changing the polarization angle.